

Research Article

Open Access



# Tuning Ag<sup>+</sup> and Mn<sup>2+</sup> doping in ZnS:Ag,Mn embedded polymers for flexible white light emitting films

Lun Ma<sup>1</sup>, Eric Amador<sup>1</sup>, George S. Belev<sup>2</sup>, Chhabindra Gautam<sup>3</sup>, Weidong Zhou<sup>3</sup>, J. Ping Liu<sup>1</sup>, Ramaswami Sammynaiken<sup>2,\*</sup>, Wei Chen<sup>1,4,\*</sup> 

<sup>1</sup>Department of Physics, University of Texas at Arlington, Arlington, TX 76013, USA.

<sup>2</sup>Saskatchewan Structural Sciences Centre, University of Saskatchewan, Saskatoon S7N 5C9, Saskatchewan, Canada.

<sup>3</sup>Department of Electrical Engineering, University of Texas at Arlington, Arlington, TX 76013, USA.

<sup>4</sup>School of CHIPS, Xi'an Jiaotong-Loverpool University, Suzhou 215123, Jiangsu, China.

\* **Correspondence to:** Prof. Wei Chen, Department of Physics, University of Texas at Arlington, 502 Yates Street, Arlington, TX 76013, USA. E-mail: weichen@uta.edu; Dr. Ramaswami Sammynaiken, Saskatchewan Structural Sciences Centre, University of Saskatchewan, 107 Wiggins Road, Saskatoon S7N 5C9, Saskatchewan, Canada. E-mail: r.sammynaiken@usask.ca

**How to cite this article:** Ma L, Amador E, Belev GS, Gautam C, Zhou W, Liu JP, Sammynaiken R, Chen W. Tuning Ag<sup>+</sup> and Mn<sup>2+</sup> doping in ZnS:Ag,Mn embedded polymers for flexible white light emitting films. *Soft Sci* 2024;4:1. <https://dx.doi.org/10.20517/ss.2023.32>

**Received:** 22 Jul 2023 **First Decision:** 17 Aug 2023 **Revised:** 10 Nov 2023 **Accepted:** 23 Nov 2023 **Published:** 4 Jan 2024

**Academic Editors:** Zhifeng Ren, Chuanfei Guo **Copy Editor:** Pei-Yun Wang **Production Editor:** Pei-Yun Wang

## Abstract

Flexible Light Emitting Diodes are versatile lighting solutions that offer bendable and adaptable illumination possibilities. A soft, flexible white luminescent film (1 mm) shows promise for foldable electroluminescent devices and applications. This film was fabricated using ZnS:Ag and Mn. Under different excitation wavelengths, the phosphors emit blue light due to Ag<sup>+</sup> luminescence centers and red light from the d-d transition of Mn<sup>2+</sup>. The blue emission is greatly suppressed at high Mn<sup>2+</sup> doping levels, requiring reduced Ag<sup>+</sup> doping in co-doped ZnS:Ag,Mn compared to solo-doped ZnS:Ag samples. By adjusting Ag<sup>+</sup> and Mn<sup>2+</sup> concentrations, the ZnS:Ag(1%),Mn(0.2%) phosphors show a proper intensity ratio of blue and red emissions, making them a promising candidate for future white light applications.

**Keywords:** Flexible, ZnS:Ag, Mn, nanoparticles, thin films, luminescence, LEDs

## INTRODUCTION

Flexible electronic devices represent a groundbreaking technological advancement, enabling the creation of lightweight, bendable components with a wide array of applications. For example, it enables the



© The Author(s) 2024. **Open Access** This article is licensed under a Creative Commons Attribution 4.0 International License (<https://creativecommons.org/licenses/by/4.0/>), which permits unrestricted use, sharing, adaptation, distribution and reproduction in any medium or format, for any purpose, even commercially, as long as you give appropriate credit to the original author(s) and the source, provide a link to the Creative Commons license, and indicate if changes were made.



development of curved or rollable screens, enhances user experiences, and increases design possibilities for TVs and displays. Most importantly, foldable and flexible electronic devices are designed with the ability to bend, curve, or fold without compromising their functionality. These devices utilize innovative materials and engineering techniques to achieve their flexibility, allowing for seamless integration into various applications. Foldable and flexible devices offer significant advantages such as portability, durability, and versatility. They can be folded or rolled up, making them compact and easy to carry. In cell phones and other mobile devices, flexible electronics contribute to sleeker and more durable designs. Furthermore, they play a pivotal role in communications by enabling compact, high-performance antennas and sensors, such as flexible piezoelectric generators and electronics, for wearable health monitoring<sup>[1,2]</sup>. They represent a promising frontier in the evolution of electronic devices, enabling new possibilities for design and user experience<sup>[3-5]</sup>. In the realm of artificial intelligence (AI), flexible electronic components facilitate the development of wearable devices, expanding the scope of data collection and interaction possibilities. These devices may also find applications in sectors such as consumer electronics, wearable technology, healthcare, and more.

Flexible Light Emitting Diodes (LEDs) are a key element for solid-state displays and foldable electronic devices<sup>[3-6]</sup>. In this research article, we present white light-emitting flexible films for displays by using Polydimethylsiloxane (PDMS) substrate embedded with Ag<sup>+</sup> and Mn<sup>2+</sup> co-doped (ZnS:Ag,Mn) phosphors. Zinc Sulfide (ZnS) is a wide bandgap semiconductor that has been extensively studied for its optical properties, low cost, durability, and low toxicity<sup>[7-15]</sup>. When doped with different elements such as Mn, Cu, Co, Eu, and Ag, they show different and unique characteristic emissions. For example, ZnS:Mn, Eu<sup>[9,10,16]</sup> and ZnS:Ag, Co<sup>[13]</sup> exhibit strong white luminescence, while the emissions of ZnS:Eu<sup>2+</sup> are highly determined by the particle size<sup>[17]</sup>. These properties offer excellent insight into adjusting the materials for different applications such as full-color displays for flexible electronics<sup>[18]</sup>.

Here, we use simple diffusion to produce a white light-emitting mixture of ZnS (Ag,Mn) by varying the amounts (percentages) of silver and manganese dopants to an optimal level. Flexible films were fabricated using a PDMS substrate embedded with ZnS:Ag,Mn phosphors, which, upon excitation with a UV LED, produced white light emissions. In this work, ZnS:Ag:Mn nanoparticles were synthesized and embedded in a flexible film for the first time and used for LED fabrication based on UV Chips. The physical properties and the luminescence behaviors, including the doping concentration dependence, temperature and luminescence decays, were systemically investigated.

## EXPERIMENTAL AND CHARACTERIZATION METHOD

### Synthesis

ZnS (99.99%), manganese chloride (MnCl<sub>2</sub>, 99%), and silver chloride (AgCl, 99.9%) were purchased from Sigma-Aldrich in the USA. All the chemicals were used as obtained. The ZnS:Mn, Ag, ZnS:Mn (Mn-doped ZnS), and ZnS:Ag phosphors are prepared using solid-state diffusion methods. Briefly, calculated amounts of ZnS, MnCl<sub>2</sub>, and/or AgCl were ground together thoroughly and loaded into ceramic crucibles. The crucibles were then embedded in carbon charcoal and sintered at 800 °C for 3 h before cooling to room temperature.

### Characterization

The identity, crystalline structure, and size of the ZnS:Ag,Mn phosphors were determined by X-ray diffraction (XRD), scanning electron microscopy (SEM), and transmission electron microscopy (TEM). Energy dispersive X-ray spectroscopy (EDS) was used to carry out the chemical characterization. The X-ray powder diffraction was recorded in a Bruker D8 X-ray diffractometer with a radiation beam of  $\lambda = 1.5406 \text{ \AA}$ .

The ZnS:Ag,Mn phosphors were first dispersed in pure water and then placed onto holey carbon-covered copper grids for TEM observations. The TEM and SEM images and EDS spectra of the particles were obtained with a Hitachi 9500 electron microscope with an accelerating voltage of 300 kV. The photoluminescence spectra were measured by using a Shimadzu RF-5301PC fluorescence spectrophotometer.

The decay lifetime data was acquired using a 355 nm pulsed laser source DPLS-355/30, Rapp Optoelectronic GmbH as an excitation source having a pulse duration of 1 ns FWHM. A CM112 monochromator, Spectral Products, was used to select the observation wavelength. A cooled photomultiplier detector head, PMC-100, Becker & Hickl GmbH, connected to a gated photon counter SR400, Stanford Research System, was used to record the decay curves.

## RESULTS AND DISCUSSIONS

### Structure

ZnS forms a sphalerite ( $\beta$ -ZnS) or wurtzite ( $\alpha$ -ZnS) structure, depending on the synthesis conditions such as reaction temperatures and precursor concentrations. To reveal the effect of Ag and/or Mn doping on ZnS crystal structures, the pure, as purchased, ZnS was also calcined at the same condition as other samples for comparison. **Figure 1** shows the XRD patterns of ZnS, ZnS:Ag(1%), ZnS:Mn(1%), and ZnS:Ag(1%),Mn(1%) samples. Both sphalerite and wurtzite structures have been observed in all the synthesized samples. The displayed diffraction peaks fit very well with standard XRD peak positions of pure sphalerite ZnS (JCPDS, No. 05-0566) and wurtzite ZnS (JCPDS, No. 36-1450), which were indexed and shown with their lattice planes in **Figure 1A**. A portion of the XRD patterns of the sample is enlarged [**Figure 1B**] and shows that the diffraction peaks of Ag<sup>+</sup> and/or Mn<sup>2+</sup>-doped samples have shifted to the left-hand side compared to the ZnS sample with no doping. The observation of the XRD peak shifting of doped samples is expected. Since the ion radius of Ag<sup>+</sup> (1.26 Å) or Mn<sup>2+</sup> (0.83 Å) is larger than Zn<sup>2+</sup> (0.74 Å)<sup>[19,20]</sup>, successful Ag<sup>+</sup> and/or Mn<sup>2+</sup> doping can enlarge the lattice parameter of ZnS. Compared to the Ag<sup>+</sup> or Mn<sup>2+</sup> doping along (ZnS:Ag or ZnS:Mn), the diffraction peaks from the ZnS:Ag,Mn sample display the largest shift. Additionally, there are two more wurtzite structure peaks appearing [W(101) and W(103)]. The W(101) peak is much more intense in the ZnS:Ag,Mn sample than in the ZnS sample, indicating that the co-doping of Ag<sup>+</sup> or Mn<sup>2+</sup> results in more wurtzite phase. For the Ag<sup>+</sup> or Mn<sup>2+</sup> solo-doped ZnS:Ag and ZnS:Mn samples, there are no other differences except for the previously discussed diffraction peak shifts observed when compared to the ZnS sample.

### Morphology

**Figure 2A** displays a typical SEM image of ZnS:Ag,Mn phosphors. The average diameter of the ZnS:Ag,Mn particles was estimated to be 4~5  $\mu$ m. Interestingly, in the high-magnification SEM image [**Figure 2B**], smaller particles are observed on these large ZnS:Ag,Mn particle surfaces. High resolution electron transmission microscopy (HRTEM) was further conducted and focused on the smaller particles. The HRTEM image [**Figure 2C**] clearly shows the existence of small spherical particles that are about 0.5  $\mu$ m. The EDS measurement on these small particles confirms that they are composed of Zn and S [**Figure 2D**]. Low levels of Cu, C, and O can be seen due to the copper grid sample holder composition. These elements are common impurities in sample preparation. Due to their low doping concentrations, neither Ag nor Mn was observed. A co-existence of large (4~5  $\mu$ m) and small (~0.5  $\mu$ m) ZnS:Ag,Mn particles may have been established in this material. From the SEM and TEM observation, it is probable that the formation of larger ZnS:Ag,Mn particles results from the aggregation of smaller particles.

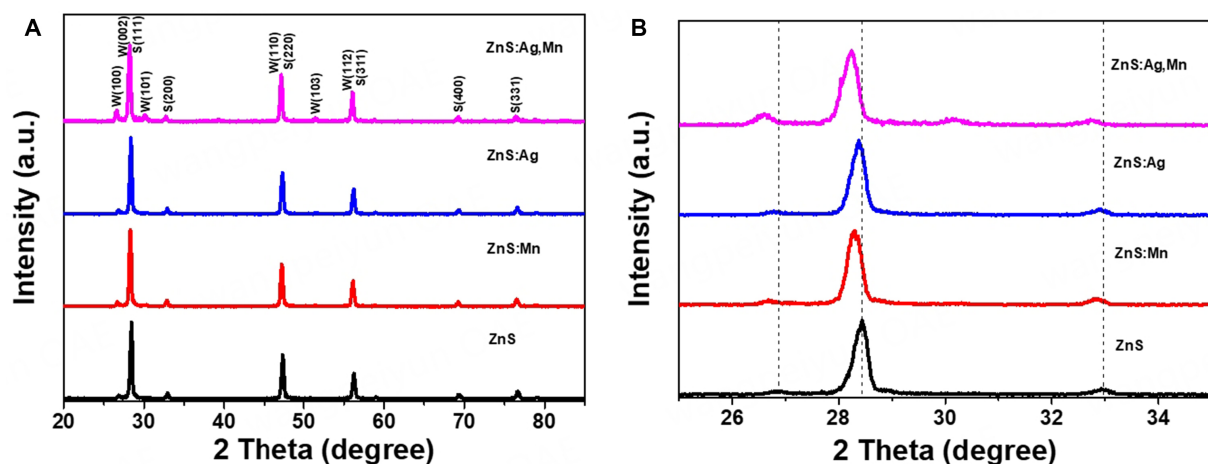


**Figure 1.** XRD patterns of the ZnS, ZnS:Ag, ZnS:Mn, and ZnS:Ag,Mn samples. Both sphalerite and wurtzite structures are observed (A). The plot (B) is an enlarged portion of the XRD patterns displaying the peak shifting due to  $\text{Ag}^+$  and/or  $\text{Mn}^{2+}$  doping. XRD: X-ray diffraction.

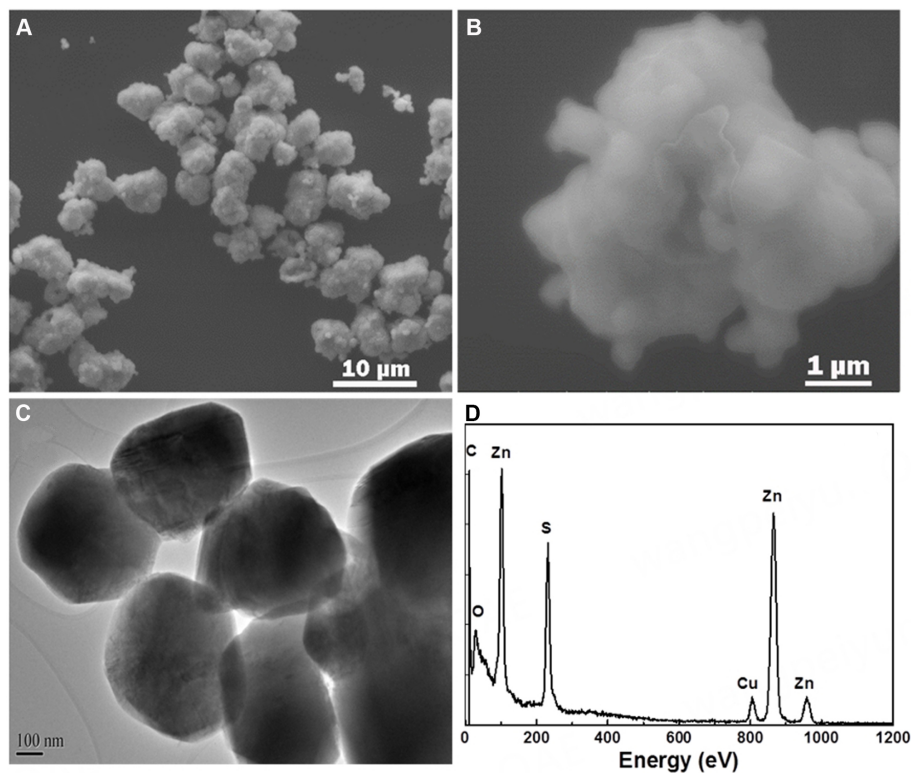


**Figure 2.** SEM images (A) and (B) and TEM image (C) display the co-existence of large (4-5  $\mu\text{m}$ ) and small ( $\sim 0.5 \mu\text{m}$ ) particle sizes of ZnS:Ag,Mn phosphors. Image (D) is an EDS spectrum measured on a small particle shown in the image (C). EDS: Energy dispersive X-ray spectroscopy; SEM: scanning electron microscopy; TEM: transmission electron microscopy.

### Photoluminescence

The emission (PL) and excitation (PLE) spectra of synthesized ZnS:Ag phosphors are shown in [Figure 3](#). Blue photoluminescence from ZnS:Ag phosphors is attributed to electron transition from sulfur vacancies to Ag luminescence centers<sup>[21-23]</sup>. At multiple excitation wavelengths (330, 340, and 350 nm), ZnS:Ag phosphors display the same blue emission peaked at 450 nm but at different intensities [[Figure 3A](#)], which is

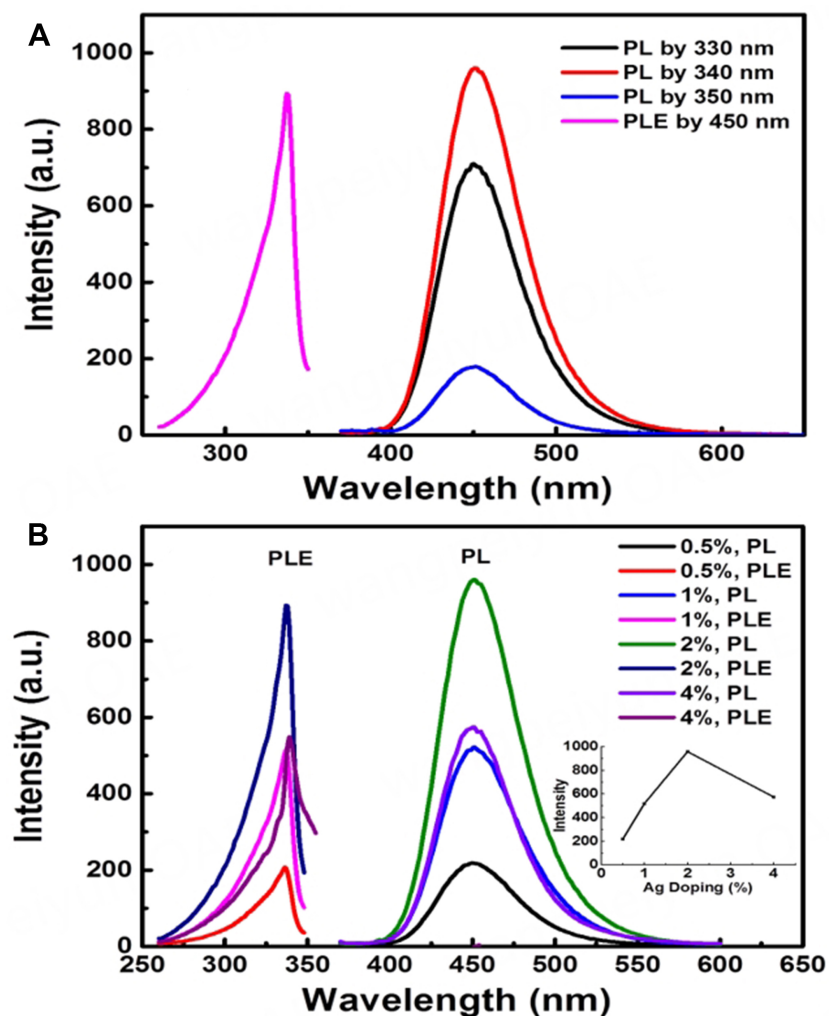


**Figure 3.** (A) The emission and excitation spectra of ZnS:Ag(2%) phosphors. The emission spectra are monitored by different excitation wavelengths; (B) The emission and excitation spectra of ZnS:Ag phosphors at different Ag<sup>+</sup> doping concentrations ( $\lambda_{\text{ex}} = 340 \text{ nm}$ ,  $\lambda_{\text{em}} = 450 \text{ nm}$ ). The inset is a plot of the ZnS:Ag emission intensities as a function of Ag<sup>+</sup> doping concentrations.

consistent with previous reports<sup>[24-28]</sup>. The excitation spectrum is narrow, peaked at about 340 nm (3.8 eV), and suggests that the band edge absorption of ZnS plays a significant role in the emission intensities observed from the excitation. Figure 3B shows the ZnS:Ag PL and PLE spectra using different Ag doping concentrations ( $\lambda_{\text{ex}} = 340 \text{ nm}$ ). It can be seen that the emission peak remains at 450 nm, but its absorption and emission intensities vary in a way that is not expected. The inset in Figure 3B reveals a relationship between the intensity of this blue emission and Ag<sup>+</sup> doping concentration. Compared to other doping concentrations, the 2% Ag<sup>+</sup> doping results in the highest absorption and fluorescence intensity.

ZnS:Mn phosphors were prepared using the same experimental conditions as the ZnS:Ag. Figure 4 shows similar optical property data for the prepared ZnS:Mn phosphors. The red emission centered at 586 nm is from the  ${}^4\text{T}_1-{}^6\text{A}_1$  transition of Mn<sup>2+</sup> ions<sup>[29-31]</sup>, while a shoulder located at about 640 nm on the emission spectrum is due to interactions of Mn<sup>2+</sup> ions [Figure 4A]. The ZnS:Mn excitation spectrum also peaked at approximately 340 nm and is attributed to the band-edge absorption of ZnS. We also prepared ZnS:Mn

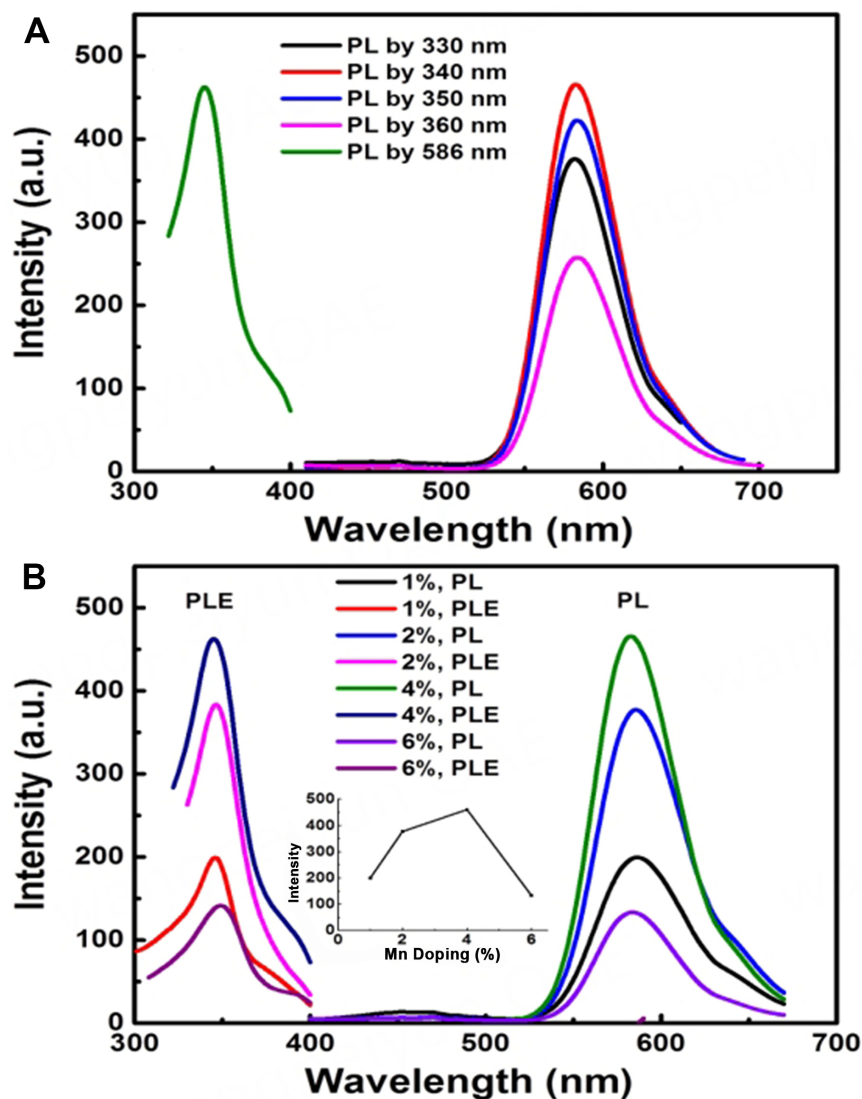


**Figure 4.** (A) The emission and excitation spectra of ZnS:Mn(4%) phosphors. The emission spectra are obtained by different excitation wavelengths; (B) The emission and excitation spectra of ZnS:Mn phosphors at different Mn<sup>2+</sup> doping concentrations ( $\lambda_{\text{ex}} = 340$  nm,  $\lambda_{\text{em}} = 586$  nm). The inset is a plot of the ZnS:Mn emission intensities as a function of Mn<sup>2+</sup> doping concentrations. The intensity is reduced at a factor of 1/3 in measurement.

samples by varying Mn doping concentrations to determine an optimized Mn<sup>2+</sup> concentration, which may lead to the most intense red emission in solo-doped ZnS:Mn phosphors. Figure 4B shows that the ZnS:Mn phosphor emits the highest red luminescence when Mn<sup>2+</sup> is doped at 4%. A weak blue band (when Mn = 1%) is observed and assigned to defect luminescence centers<sup>[32]</sup>. However, its contribution would be insignificant since it is very weak and disappears quickly as the Mn<sup>2+</sup> doping concentration increases.

It was seen that both ZnS:Ag and ZnS:Mn are excited by ZnS band-edge absorption and emit intense fluorescence. Moreover, as the Ag<sup>+</sup> blue emission and Mn<sup>2+</sup> red emission cover from violet to green (400~560 nm) and green to red (540 to 680 nm) in luminescence spectra, it presents the opportunity to investigate Ag and Mn co-doped ZnS (ZnS:Ag,Mn) phosphors for white light production. Considerations of possible quenching effect at high Ag and/or Mn concentrations were addressed by preparing ZnS:Ag,Mn

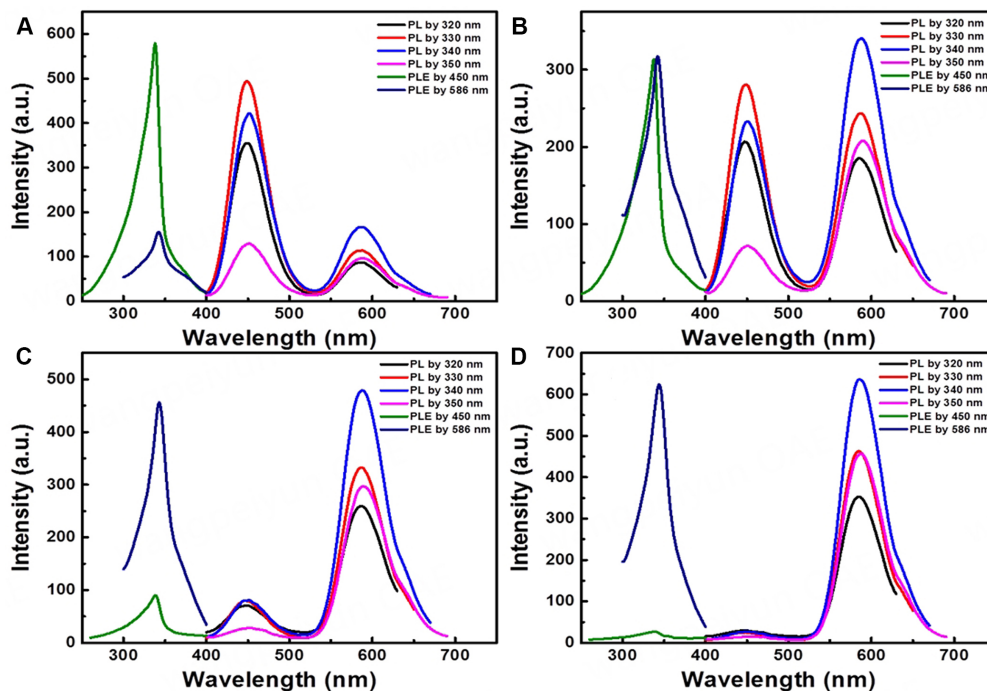


**Figure 5.** The emission and excitation spectra of ZnS:Ag(0.5%),Mn monitored by different wavelengths. The doping concentration of Mn<sup>2+</sup> is (A) 0.1%, (B) 0.2%, (C) 0.5%, and (D) 1.0%, respectively.

samples at a relatively low Ag concentration of 0.5% and varied co-doped Mn concentration from 0.1% to 1%. The photoluminescence spectra of the samples prepared are revealed in Figure 5. Under different excitation wavelengths from 320 to 350 nm, all the samples show both blue and red emission peaks at the same fluorescence wavelengths as displayed in solo-doped ZnS:Ag and ZnS:Mn samples. Therefore, transitions can be assigned to the same luminescence mechanisms previously discussed, i.e., two-electron transition pathways emitting blue and red light. The blue emission was assigned to be from defects to Ag<sup>+</sup> luminescence centers, the other from the Mn<sup>2+</sup> d-d transition (<sup>4</sup>T<sub>1</sub>-<sup>6</sup>A<sub>1</sub>). With a fixed Ag<sup>+</sup> doping concentration of 0.5%, Figure 5A-D displays the emission and excitation spectra of ZnS:Ag,Mn samples when Mn<sup>2+</sup> doping were 0.1%, 0.2%, 0.5%, and 1%, respectively. It was observed that the blue emission was significantly quenched when Mn doping was relatively high (0.5% Mn or 1% Mn). Particularly, the blue emission due to Ag luminescence centers almost disappeared at 1% Mn<sup>2+</sup> co-doping, while the red emission due to Mn<sup>2+</sup> doping showed similar intensity in comparison to the solo-doped ZnS:Mn(1%). This evidence revealed that the Mn<sup>2+</sup> d-d transition must take precedence in the two-electron transition pathways and can suppress the transition from defects to Ag luminescence centers. In consequence, the Mn concentration may need to be kept at low levels to have an intensive Ag<sup>+</sup> blue emission in co-doped ZnS:Ag,Mn phosphors. Here, the blue emission was more intense for the samples with lower Mn concentrations of both 0.1% and 0.2%. However, the red emissions in the Mn(0.1%) sample were much weaker than the Mn(0.2%) sample under different excitation wavelengths. Considerations from the above characteristics led to the ZnS:Ag(0.5%),Mn(0.2%) phosphors being selected as a white light emitting candidate for further investigation.

Figure 6 reveals the intensities of ZnS:Ag(0.5%),Mn(0.2%) blue and red emissions using different excitation wavelengths. The intensity ratio of the average blue emission (450 nm) to red emission (586 nm) showed to be about 0.8 and suggested that the ZnS:Ag(0.5%), Mn(0.2%) overall blue emission was less intensive than its red emission when a practical excitation source was used. Hence, it would be necessary to increase the blue emission intensity in the ZnS:Ag(0.5%),Mn(0.2%) phosphor for white light applications. For further

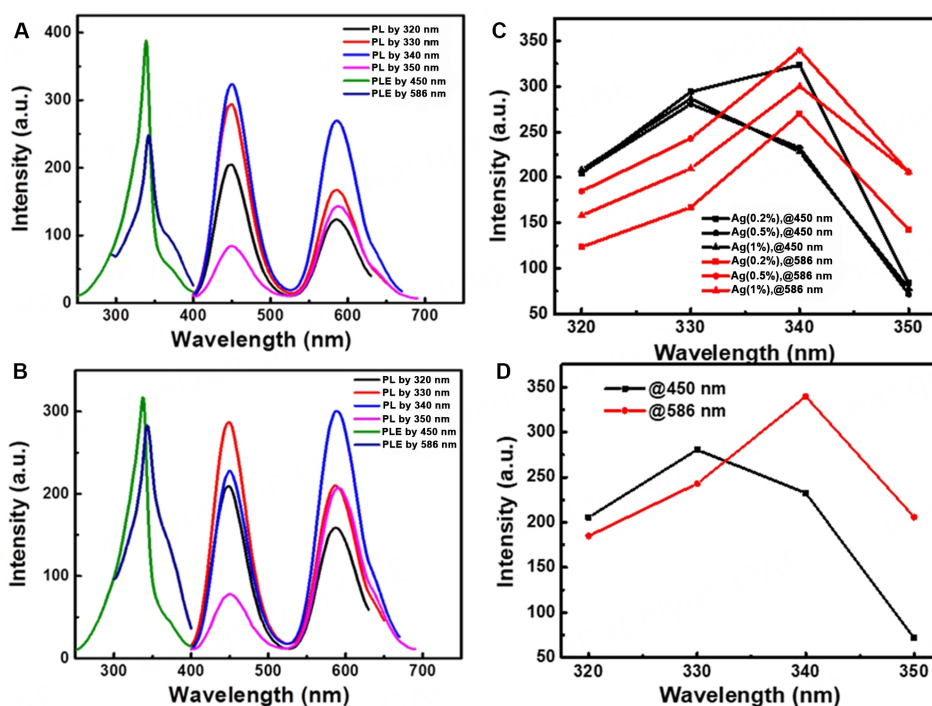


**Figure 6.** (A) and (B) The intensities of ZnS:Ag(0.5%), (0.2%) blue (450 nm) and red (586 nm) emissions under different excitation wavelengths; (C) The emission spectra of ZnS:Ag(0.2%),Mn(0.2%), ZnS:Ag(0.5%),Mn(0.2%) and ZnS:Ag(1%),Mn(0.2%) monitored by different wavelengths; (D) The intensities of ZnS:Ag,Mn blue (450 nm) and red (586 nm) emissions under different excitation wavelengths when Ag<sup>+</sup> doping concentration is 0.2%, 0.5%, and 1%, respectively. The Mn<sup>2+</sup> concentration is 0.2% for all the samples.

investigation, ZnS:Ag(0.2%),Mn and ZnS:Ag(1%),Mn phosphors were prepared with varying Mn concentrations (0.1%, 0.2%, 0.5%, and 1%). Similarly, at 0.1% Mn<sup>2+</sup> doping, the red emission was much weaker than the blue emission so that it was not proper for white light applications. As for the 0.5% or 1% Mn<sup>2+</sup> doping, the red emission was much more intensive than the blue emission, as was seen for the ZnS:Ag(0.5%),Mn(0.5%) and ZnS:Ag(0.5%),Mn(1%) samples discussed in Figure 5. Figure 6 displays the emission and excitation spectra of ZnS:Ag(0.2%),Mn(0.2%), ZnS:Ag(0.5%),Mn(0.2%), and ZnS:Ag(1%),Mn(0.2%) phosphors. Compared to the ZnS:Ag(0.5%),Mn(0.2%) sample, the blue and red emissions from the ZnS:Ag(0.2%),Mn(0.2%) sample are getting stronger and weaker, respectively [Figure 6A], while the emissions from ZnS:Ag(1%),Mn(0.2%) seem to remain at similar intensities [Figure 6B]. In order to figure out the best candidate for white light applications, the intensities of blue (450 nm) and red (586 nm) emissions from ZnS:Ag,Mn phosphors under different excitation wavelengths are plotted together with varying Ag<sup>+</sup> doping concentrations (0.2%, 0.5%, and 1%), as shown in Figure 6C and D. The Mn<sup>2+</sup> concentration is fixed at 0.2% for all the samples. Unlike the solo-doped ZnS:Ag phosphors, the most intensive blue emission is found when Ag is at 0.2%, indicating that Ag<sup>+</sup> concentration quenching has occurred at a significantly lower concentration level in the presence of Mn<sup>2+</sup> ions. On the other hand, it is seen that the red emissions from ZnS:Ag(0.2%),Mn(0.2%) are weaker than from the ZnS:Ag(0.5%),Mn(0.2%) and ZnS:Ag(1%),Mn(0.2%) samples. This is reasonable due to its high blue emission. The ratio of average blue/red emission intensities of the ZnS:Ag(0.2%),Mn(0.2%) is found to be 1.29 with different excitation wavelengths. In comparison to the ZnS:Ag(0.5%),Mn(0.2%) phosphor, the increased Ag concentration in ZnS:Ag(1%),Mn(0.2%) has almost no change on the blue emission intensities but has reduced the red emission intensities. Calculated in the same method, the ratio of average blue/red emission intensities of the ZnS:Ag(1%),Mn(0.2%) is 0.92. Thus, the blue and red emissions from the ZnS:Ag(1%),Mn(0.2%) phosphor have closer intensities, and this sample is more appropriate for white light generation in our study.

The Commission Internationale de l' Elclairage (CIE) chromaticity coordinates of the ZnS:Ag(1%),Mn(0.2%) phosphor by varying excitation wavelengths are displayed in [Figure 7](#). We can find that the test chromaticity coordinates corresponding with excitation wavelengths 320 and 330 nm are located in the white light region. With the increase of excitation wavelength from 320 to 340 nm, the emission color shifts from bluish white light to reddish white light. Although the 350 nm excitation generates chromaticity coordinates in a more reddish region, its emission intensity is much lower than that using excitation wavelengths from 320 to 340 nm due to the sharp ZnS:Ag,Mn excitation bands. The inset in [Figure 7](#) displays a photo image of ZnS:Ag(1%),Mn(0.2%) under a UV lamp with an emission peak at 365 nm, which shows the overall white light output from the ZnS:Ag(1%),Mn(0.2%) and the images of flexible ZnS:Ag(1%),Mn(0.1%) infused PDMS. The right chromaticity plot shows the color of the samples listed in [Table 1](#).

### Quantum yield

External photoluminescent quantum yield (EQY) measurements were performed using a Thorlabs integrating sphere to observe the changes in emission yield as different dopant concentrations of Ag<sup>+</sup> and Mn<sup>2+</sup> were varied in the ZnS. The chosen samples were mixed in PDMS polymers and placed onto a quartz slide of 1 cm<sup>2</sup> area, each containing 15 mg of sample mass. Samples were then cured at 125 °C for 30 min until solid. A 365 nm UV-LED pen was used as an excitation source to measure the EQY. EQY was calculated as follows:

$$EQY = \frac{A_1}{A_0}$$

Where A<sub>1</sub> is the sum of the photon counts from 400-700 nm (emission), and A<sub>0</sub> is the sum of the photon counts from 350-400 nm (incident). The EQY of ZnS:Mn, ZnS:Ag, and ZnS:Ag,Mn Phosphors are shown in [Table 2](#).

### Photoluminescence decay lifetime

The Photoluminescence Decay (PLD) measurements were conducted at room temperature on four samples of ZnS:2%Ag with different Mn doping levels: 0.1%, 0.2%, 0.5%, and 1%, respectively [[Figure 8A](#)]. As can be seen from [Figure 8B](#) and [C](#), the PLD curves that were recorded at 450 and 590 nm occur on very different time scales. The average lifetime for the 450 nm emission was measured at around 1 μs, while for the 590 nm region, the average lifetime was approximated at more than three orders of magnitude longer (several ms). This means that 10 μs after the end of the excitation pulse, all the light emitted by the samples was in the region centered on 590 nm, in agreement with the data about similar samples<sup>[24-28]</sup>. Most researchers usually associate the prompt luminescence (450 nm region) in ZnS:Ag powdered scintillators with excitonic recombination. The initial part of the decay can be fitted with two exponentials, and that suggests that two types of recombination centers with different oscillator strengths would be involved in the process<sup>[20,21]</sup>. The decay constants of 26 ns and 130 ns were previously reported<sup>[20,21]</sup>. In our experiments [[Figure 8B](#)], the first decay constant was outside of our experimentally accessible time scale. For the second time constant, we measured a value of 122 ns, which is close to the reported values<sup>[20,21]</sup>. The fast initial decay in the 450 nm region was followed by an afterglow governed by different electron and hole traps present in the material. This part of the decay can be approximated with a hyperbolic function or, in simple cases, by an exponential function<sup>[20]</sup>. We chose to fit the afterglow to a single exponential function, which was appropriate due to the short time scale of our experiment. The afterglow decay constant value of 1μs that we

**Table 1. The color temperatures of ZnS:Mn, ZnS:Ag, and ZnS:Ag,Mn phosphors**

Sample	X	Y	Color temp (K)
2% Mn	0.40468	0.39184	3,526
2% Ag, 0.1% Mn	0.23859	0.21097	102,911
1% Ag	0.19938	0.15891	6,845
1% Ag, 0.1% Mn	0.30144	0.30007	7,618
1% Ag, 1% Mn	0.39379	0.36095	3,526

**Table 2. The EQY of ZnS:Mn, ZnS:Ag, and ZnS:Ag,Mn phosphors**

Doping %	2% Mn	2% Ag, 0.1% Mn	Ag 1%	1% Ag, 0.1% Mn	1% Ag, 1% Mn
EQY	8.5%	21.0%	41.0%	3.6%	10.9%

EQY: External photoluminescent quantum yield.

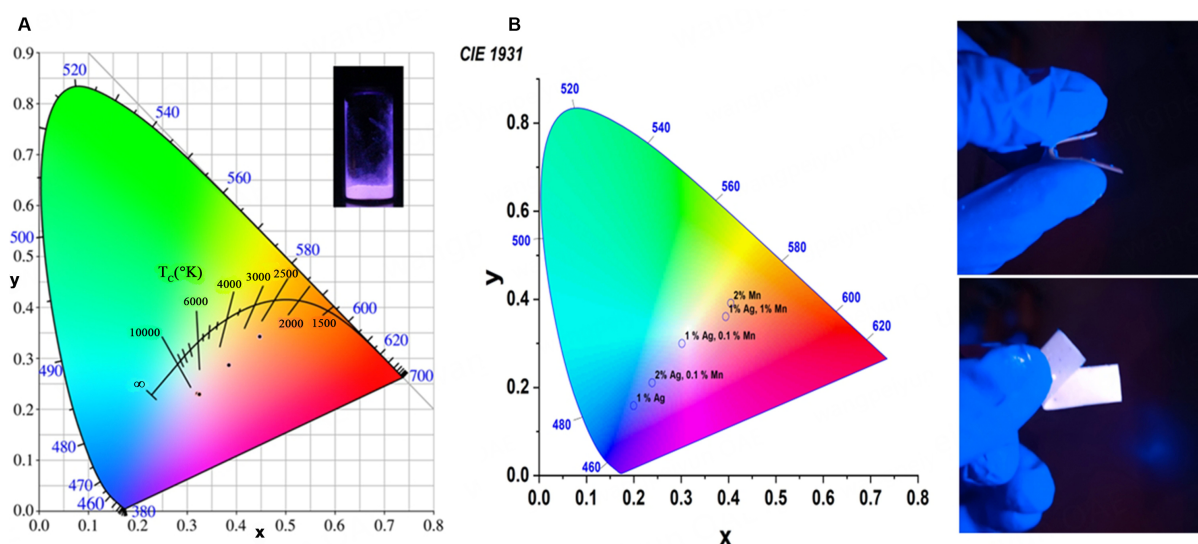


**Figure 7.** (A) The CIE chromaticity coordinates (displayed as dark dots from left to right hand side) of ZnS:Ag(1%),Mn(0.2%) under different excitation wavelengths at 320, 330, 340, and 350 nm, respectively. The left inset is a photo image of ZnS:Ag(1%),Mn(0.2%) under a UV lamp (peaked at 365 nm); (B) CIE coordinates of samples in Table 1. Far right: Images of flexible ZnS:Ag(1%),Mn(0.1%) infused PDMS. CIE: Commission Internationale de l' Elclairage; PDMS: polydimethylsiloxane.

obtained [Figure 8B] was in good agreement with the data published<sup>[20]</sup>.

The photoluminescence in the 590 nm region has been associated with the Mn<sup>2+</sup> ions. A characteristic feature of the Mn<sup>2+</sup> emission is the long decay lifetime (up to several milliseconds) due to the spin-forbidden <sup>4</sup>T<sub>1</sub>-<sup>6</sup>A<sub>1</sub> d-d transitions<sup>[24-26]</sup>, whereas the presence of defects could shorten the decay lifetime<sup>[24]</sup>.

In practice, it is hard to disperse the Mn homogeneously in the material and to keep the coordination of the Mn ions the same (always substitutional doping). For that reason, in most systems, the decay kinetics is complicated due to the presence of magnetic coupling between the Mn<sup>2+</sup> ions in the material and/or due to Mn<sup>2+</sup> ions residing on the surface of the powder particle, which can be easily observed at high doping concentrations and/or hosts containing particles with small size. Thus, it is difficult to assign decay channels to different light-emitting Mn<sup>2+</sup> species because Mn<sup>2+</sup> ions with different degrees of coupling may generate

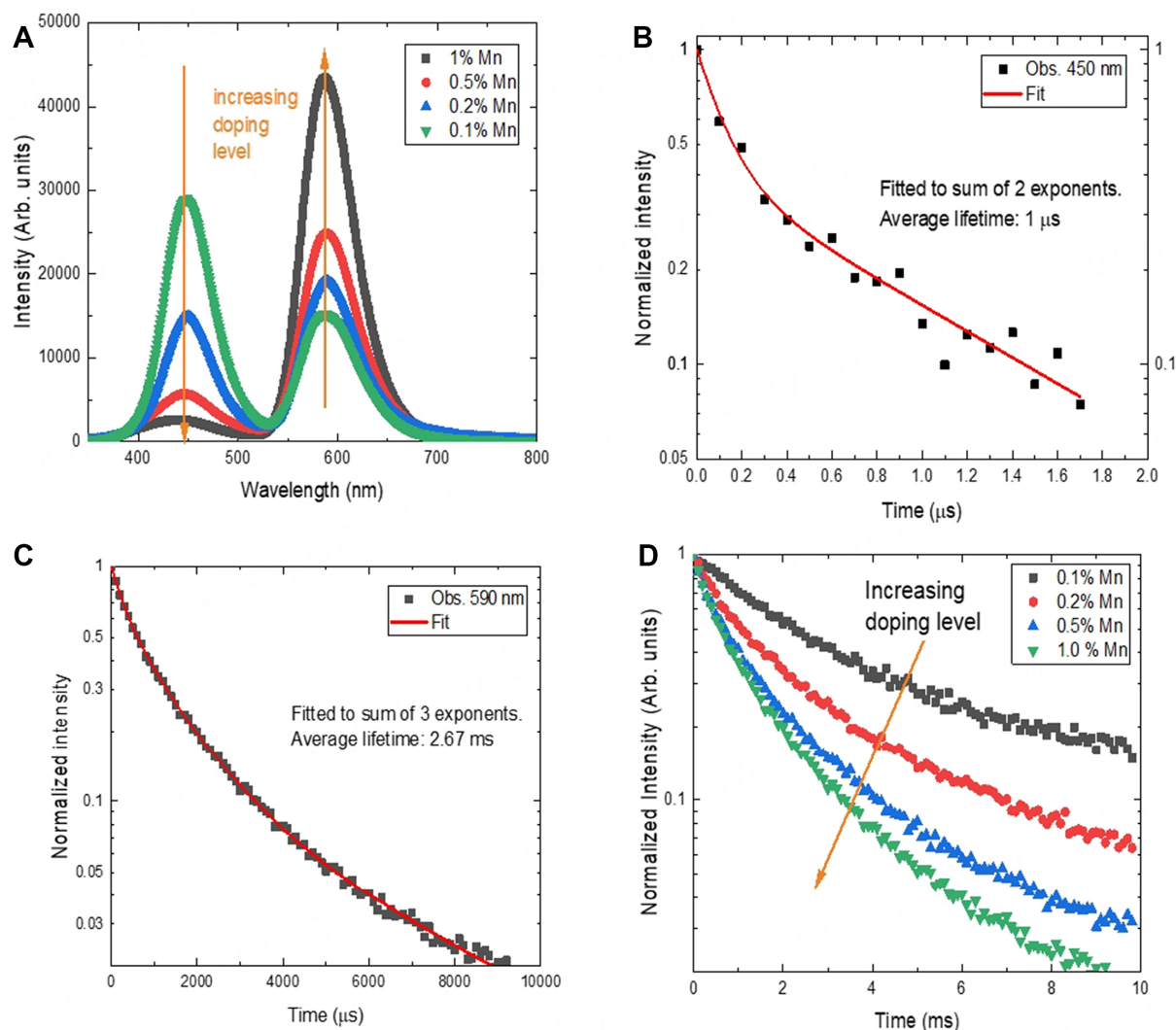


**Figure 8.** (A) The emission spectra of ZnS:2%Ag samples containing 0.1%, 0.2%, 0.5%, and 1.0% Mn excited by 355 nm laser pulses with duration of 1 ns and 10 kHz repetition rate; (B) Emission decay curve for ZnS:2%Ag:1%Mn recorded with 450 nm observation wavelength at a 20 Hz repetition rate; (C) Emission decay curve for ZnS:2%Ag:1%Mn recorded with an observation wavelength of 590 nm and a 10 Hz repetition rate; (D) Dependence of the emission decay at 590 nm on the level of Mn doping. Measurements are done at a 10 Hz repetition rate.

numerous relaxation pathways. In most cases, the decay can be fitted reasonably well to the sum of three exponentials, and we chose that approach for our experimental data [Figure 8C and Table 3].

For the reasons mentioned above, the decay lifetime is strongly dependent on the average distance between the Mn<sup>2+</sup> ions and decreasing that distance, i.e., by increasing the Mn concentration, leads to shortening of the observed decay lifetimes. As seen in Figure 8D and Table 3, the observed decay constants are inversely proportional to Mn dopant concentrations, which is in good agreement with previously published research<sup>[33,34]</sup>.

Actually, not only the decay lifetimes but also the luminescence efficiency or intensity are highly dependent on the doping concentrations as can be seen in Figure 8A. Further, the ZnS:Ag with 2% Mn has the strongest luminescence in intensity. Usually, at low concentrations, the luminescence intensity is increased

**Table 3. The lifetimes of the individual components in ZnS:Ag(2%),Mn(x) phosphors**

Mn content, %	$A_1$	$\tau_{1r}$ ms	$A_2$	$\tau_{2r}$ ms	$A_3$	$\tau_{3r}$ ms	$\tau_{avg}$ ms
0.1	0.19	1.9	0.53	1.7	0.27	17.6	13.7
0.2	0.23	0.4	0.58	1.7	0.19	8.8	6
0.5	0.22	0.2	0.6	1.2	0.18	5.3	3.4
1.0	0.28	0.3	0.58	1.2	0.13	4.6	2.7

with the increasing concentrations; when it reaches the peak, the intensity is decreased with further increasing the concentration as a result of concentration quenching, as reported in other publications<sup>[10,35]</sup>. However, the critical concentration for this kind of quenching is higher, which makes it possible to reach higher efficiency in doped nanophosphors<sup>[10,36]</sup>.

The research on ZnS:Mn,Ag nanoparticles for foldable LEDs represents a novel and groundbreaking contribution to the field of nanotechnology and optoelectronics. While extensive work has been conducted on ZnS-based nanoparticles, the introduction of manganese and silver dopants into the ZnS matrix is a unique and innovative approach that has not been extensively explored. This novel combination of materials opens up new possibilities for enhancing the performance and functionality of LEDs.

Moreover, the incorporation of ZnS:Mn,Ag nanoparticles, specifically for foldable LEDs, is a pioneering concept that, to the best of our knowledge, has not been previously reported in the literature. The development of foldable LEDs is of significant interest due to the increasing demand for flexible and portable display technologies. This research not only offers a new avenue for achieving foldable LEDs but also addresses the challenges and opportunities associated with this emerging technology.

The study of ZnS:Mn,Ag nanoparticles for foldable LEDs represents a unique and unexplored dimension in the field of nanomaterials and optoelectronics. By investigating this uncharted territory, this research promises to advance our understanding of materials science and potentially lead to the development of innovative, flexible, and high-performance lighting devices with a wide range of applications in the display industry.

Here, we present the successful synthesis of luminescent nanoparticles and their subsequent integration into flexible films, showcasing their potential applications in the development of foldable electronic devices. However, it is imperative to acknowledge that temperature and heating pose formidable challenges in this context, as elevated temperatures have the potential to significantly diminish the emission efficiency of these nanoparticles<sup>[33,34]</sup>. Addressing this critical concern is a primary focus of our research, and we are dedicated to exploring innovative solutions to mitigate the adverse effects of heating on the luminescent properties of these materials.

## CONCLUSIONS

In summary, we have created a material called ZnS:Ag,Mn phosphors that can produce white light. When exposed to the light of different colors, the ZnS:Ag,Mn phosphors emitted blue light because of defects in the Ag<sup>+</sup> luminescence centers, and the red light was attributed to Mn<sup>2+</sup> d-d transition. However, blue light dominates the emission over red, even when the concentration of Mn<sup>2+</sup> is relatively high. To prevent this, the amount of Ag<sup>+</sup> was reduced in the material when adding Mn<sup>2+</sup> to obtain the optimized white color emissions. Upon optimization of the relative concentrations of Ag<sup>+</sup> and Mn<sup>2+</sup>, it was found that the best combination was ZnS:Ag(1%),Mn(0.2%). This combination produced an optimal mix of blue and red light,

making it a good candidate for creating white light in the future. Flexible films using ZnS:Ag(1%),Mn(0.1%) are promising for possible use in foldable electroluminescent devices and applications.

## DECLARATIONS

### Authors' contributions

Conception and design of the study: Chen W, Sammynaiken R

Conducted data analysis and interpretation: Amador E, Belev GS, Chen W, Sammynaiken R, Zhou W, Liu JP

Performed data acquisition: Amador E, Belev GS, Gautam C

Provided administrative, technical, and material support: Chen W, Sammynaiken R, Zhou W

Sample synthesis and characterization: Ma L

### Availability of data and materials

Correspondence and requests for data and materials should be addressed to Chen W.

### Financial support and sponsorship

This work was supported in part by The Gap Funds from the University of Texas at Arlington.

### Conflicts of interest

All authors declared that there are no conflicts of interest.

### Ethical approval and consent to participate

Not applicable.

### Consent for publication

Not applicable.

### Copyright

© The Author(s) 2024.

## REFERENCES

1. Sun X, Zhang F, Zhang L, et al. Enhanced electromechanical conversion via in situ grown CsPbBr<sub>3</sub> nanoparticle/poly(vinylidene fluoride) fiber composites for physiological signal monitoring. *Soft Sci* 2022;2:1. DOI
2. Park C, Kim MS, Kim HH, et al. Stretchable conductive nanocomposites and their applications in wearable devices. *Appl Phys Rev* 2022;9:021312. DOI
3. Kim JH, Lee SE, Kim BH. Applications of flexible and stretchable three-dimensional structures for soft electronics. *Soft Sci* 2023;3:16. DOI
4. Wang X, Qi L, Yang H, Rao Y, Chen H. Stretchable synaptic transistors based on the field effect for flexible neuromorphic electronics. *Soft Sci* 2023;3:15. DOI
5. Nie B, Li X, Wang C, et al. Flexible double-sided light-emitting devices based on transparent embedded interdigital electrodes. *ACS Appl Mater Interfaces* 2020;12:43892-900. DOI
6. Chen W, Grouquist D, Roark J. Voltage tunable electroluminescence of CdTe Nanoparticle light-emitting diodes. *J Nanosci Nanotechnol* 2002;2:47-53. DOI
7. Ma L, Zou X, Bui B, Chen W, Song KH, Solberg T. X-ray excited ZnS:Cu,Co afterglow nanoparticles for photodynamic activation. *Appl Phys Lett* 2014;105:013702. DOI
8. Shi Y, Jiang S, Zhou K, et al. Facile preparation of ZnS/g-C<sub>3</sub>N<sub>4</sub> nanohybrids for enhanced optical properties. *RSC Adv* 2014;4:2609-13. DOI
9. Ma L, Jiang K, Liu X, Chen W. A violet emission in ZnS:Mn,Eu: luminescence and applications for radiation detection. *J Appl Phys* 2014;115:103104. DOI
10. Hossu M, Schaeffer RO, Ma L, et al. On the luminescence enhancement of Mn<sup>2+</sup> by co-doping of Eu<sup>2+</sup> in ZnS:Mn,Eu. *Opt Mater* 2013;35:1513-9. DOI
11. Qu H, Cao L, Su G, Liu W. Effect of inorganic shells on luminescence properties of ZnS:Ag nanoparticles. *J Mater Sci* 2013;48:4952-61. DOI

12. Ma L, Chen W. Enhancement of afterglow in ZnS:Cu,Co water-soluble nanoparticles by aging. *J Phys Chem C* 2011;115:8940-4. DOI
13. Ma L, Chen W. ZnS:Cu,Co water soluble afterglow nanoparticles: synthesis, luminescence and potential applications. *Nanotechnology* 2010;21:385604. DOI
14. Ma L, Chen W. Luminescence enhancement and quenching in ZnS:Mn by Au nanoparticles. *J Appl Phys* 2010;107:123513. DOI
15. Chen W, Joly AG, Zhang JZ. Up-conversion luminescence of Mn<sup>2+</sup> in ZnS:Mn<sup>2+</sup> nanoparticles. *Phys Rev B* 2001;64:412021. DOI
16. Chen W, Joly AG, Malm JO, Bovin JO. Upconversion luminescence of Eu<sup>3+</sup> and Mn<sup>2+</sup> in ZnS:Mn<sup>2+</sup>,Eu<sup>3+</sup> codoped nanoparticles. *J Appl Phys* 2004;95:667-72. DOI
17. Chen W, Malm JO, Zwiller V, et al. Energy structure and fluorescence of Eu<sup>2+</sup> in ZnS:Eu nanoparticles. *Phys Rev B* 2000;61:11021. DOI
18. Chen W. Nanophase luminescence particulate material. US Patent; 2006. Available from: <https://www.freepatentsonline.com/7067072.html>. [Last accessed on 7 Dec 2023].
19. Mann SE, Schooneveld EM, Rhodes NJ, Liu D, Sykora GJ. Timing properties of radioluminescence in nanoparticle ZnS:Ag scintillators. *Opt Mater* 2023;17:100226. DOI
20. Dai L, Torche A, Strelow C, et al. Role of magnetic coupling in photoluminescence kinetics of Mn<sup>2+</sup>-doped ZnS nanoplatelets. *ACS Appl Mater Interfaces* 2022;14:18806-15. DOI
21. Jian W, Zhuang J, Zhang D, Dai J, Yang W, Bai Y. Synthesis of highly luminescent and photostable ZnS:Ag nanocrystals under microwave irradiation. *Mater Chem Phys* 2006;99:494-7. DOI
22. Ollinger M, Craciun V, Singh RK. Nanoencapsulation of ZnS:Ag particulates with indium tin oxide for field emission displays. *Appl Phys Lett* 2002;80:1927-9. DOI
23. Hao E, Sun Y, Yang B, Zhang X, Liu J, Shen J. Synthesis and photophysical properties of ZnS colloidal particles doped with silver. *J Colloid Interf Sci* 1998;204:369-73. DOI
24. Chen W, Aguekian VF, Vassiliev N, Serov AY, Filosofov NG. New observations on the luminescence decay lifetime of Mn<sup>2+</sup> in ZnS:Mn<sup>2+</sup> nanoparticles. *J Chem Phys* 2005;123:1247071. DOI
25. Olano EM, Grant CD, Norman TJ, Castner EW, Zhang JZ. Photoluminescence decay dynamics and mechanism of energy transfer in undoped and Mn<sup>2+</sup> doped ZnSe nanoparticles. *J Nanosci Nanotechnol* 2005;5:1492-7. DOI
26. Sapra S, Prakash A, Ghangrekar A, Periasamy N, Sarma DD. Emission properties of manganese-doped ZnS nanocrystals. *J Phys Chem B* 2005;109:1663-8. DOI
27. Shimizu KT, Woo WK, Fisher BR, Eisler HJ, Bawendi MG. Surface-enhanced emission from single semiconductor nanocrystals. *Phys Rev Lett* 2022;89:117401. DOI
28. Bol AA, Meijerink A. Doped semiconductor nanoparticles - a new class of luminescent materials? *J Lumin* 2000;87-9:315-8. DOI
29. Suyver JF, Wuister SF, Kelly JJ, Meijerink A. Synthesis and photoluminescence of nanocrystalline ZnS:Mn<sup>2+</sup>. *Nano Lett* 2001;1:429-33. DOI
30. Chen W, Westcott SL, Zhang J. Dose dependence of x-ray luminescence from CaF<sub>2</sub>: Eu<sup>2+</sup>, Mn<sup>2+</sup> phosphors. *Appl Phys Lett* 2007;91:211103. DOI
31. Smith BA, Zhang JZ, Joly A, Liu J. Luminescence decay kinetics of Mn<sup>2+</sup>-doped ZnS nanoclusters grown in reverse micelles. *Phys Rev B* 2021;62. DOI
32. Murase N, Jagannathan R, Kanematsu Y, et al. Fluorescence and EPR characteristics of Mn<sup>2+</sup>-doped ZnS nanocrystals prepared by aqueous colloidal method. *J Phys Chem B* 1999;103:754-60. DOI
33. Chen W, Su F, Li G, Joly AG, Malm JO, Bovin JO. Temperature and pressure dependences of the Mn<sup>2+</sup> and donor-acceptor emissions in ZnS:Mn<sup>2+</sup> nanoparticles. *J Appl Phys* 2002;92:1950-5. DOI
34. Su FH, Ma BS, Fang ZL, Ding K, Li GH, Chen W. Temperature behaviour of the orange and blue emissions in ZnS:Mn nanoparticles. *J Phys Condens Matter* 2002;14:12657. DOI
35. Yu JH, Kim J, Hyeon T, Yang J. Facile synthesis of manganese (II)-doped ZnSe nanocrystals with controlled dimensionality. *J Chem Phys* 2019;151:244701. DOI
36. Chen W. Doped nanomaterials and nanodevices. Los Angeles: American Scientific Publisher; 2009. Available from: <http://www.aspbs.com/doped.htm>. [Last accessed on 7 Dec 2023].